Journal of Radioanalytical and Nuclear Chemistry
https://doi.org/10.1007/s10967-025-10555-8

# The use of irradiation for production of oligochitosan conjugated with graphene oxide

**Karina de Oliveira Gonçalves[1] · Miguel Duarte[1] · Daniel Perez Vieira[2] · Sumair Gouveia Araújo[3] · Liliane Landini[3] · Solange Kazumi Sakata[1]**

Received: 23 June 2025 / Accepted: 7 November 2025


**Abstract**
Chitosan and derivatives, such as oligochitosan, have been attracting significant attention in the biomedical field due to their versatility, biocompatibility, and environmental sustainability, presenting a promising alternative to synthetic materials. Obtained through the deacetylation of chitin, these biopolymers exhibit important characteristics, including biodegradability and the capacity to interact with a range of materials, which makes them suitable for a variety of applications, especially in the development of nanocomposites. The aim of this work was to obtain oligochitosans (OCH) via gamma radiation at a dose of 40 kGy, dose rate 9.8 kGy/h to functionalize graphene oxide (GO) for biomedical applications. The resulting nanocomposite (OCH/GO) was characterized by DLS, scanning microscopy and atomic force microscopy and evaluated for its cytotoxicity, demonstrating that the incorporation of the materials reduces the toxicity of GO, allowing its application in tissue engineering. The objective of this study was to produce oligochitosans (OCH) by gamma irradiation for the functionalization of graphene oxide (GO) and to assess the cytotoxicity of the resulting nanocomposite for biomedical applications. The OCH/GO nanocomposite was characterized using X-ray diffraction, scanning electron microscopy, and atomic force microscopy. Incorporation of oligochitosan reduced the intrinsic toxicity of GO, thus enhancing its potential suitability for applications in tissue engineering.

**Graphical abstract**

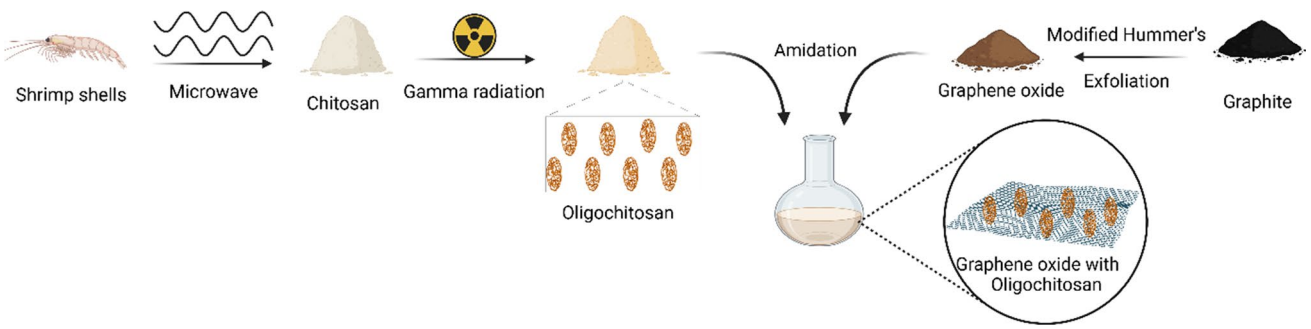


**Keywords** Chitosan · Graphene · Nanocomposites · Gamma Irradiation

## Introduction

The use of natural biopolymers has attracted significant attention in biomedical research, as they are versatile, biocompatible, and sustainable, offering a promising alternative to synthetic materials contributing to the reduction of environmental impact [1]. Among them, chitosan, (1→4)-linked 2-amido-2-deoxy-β-D-glucan, a well-known polysaccharide with unique properties including biodegradability, and antimicrobial activity [2]. It is obtained through the deacetylation of chitin, which is primarily derived from shrimp shells and other crustacean exoskeletons, materials that are often considered food-processing

Extended author information available on the last page of the article

Published online: 15 November 2025

waste [3, 4]. Its ability to interact with a wide range of materials makes it particularly suitable for diverse applications, such as membranes for wastewater treatment [5]. However, its low solubility in water and most organic solvents limits its use in biological applications [2]. To address this limitation, chemical and enzymatic degradation of chitosan chains to produce oligochitosan (OCH), an oligomeric form of chitosan, has been widely reported in the literature [6–8]. Nevertheless, these methodologies are often costly and time-consuming, and chemical approaches can generate toxic wastes. To overcome these issues, ionizing radiation has been explored as a sustainable alternative method for chitosan degradation [9]. This approach employs gamma rays or electron beams to initiate chemical reactions without the need for toxic reagents, resulting in a simplified process and high purity [10]. Chitosan degradation by gamma radiation has been reported under different pH conditions, with catalysts, and at various doses and dose rates. In this process, ionizing radiation promotes controlled polymer degradation, allowing the production of oligochitosan with well-defined sizes and physicochemical properties [11–13]. Choi et al (2002) investigated the degradation of chitosan using gamma radiation at doses ranging from 2 to 200kGy and demonstrated that the highest solubility of the oligochitosan was achieved at a dose of 40kGy [14]. Due to its water solubility and reduced viscosity, oligochitosan can be applied in a wide range of biomedical fields, including drug delivery, wound healing, tissue engineering, and antimicrobial treatments [15–17]. In addition, chitosan and its oligomers exhibit the ability to coat metallic nanoparticles, acting not only as stabilizers but also influencing nanoparticle morphology through shape-directing and size-controlling mechanisms [18]. They can also act as grafting agents for polymers, leading to a reduction in the cytotoxicity of these materials [19]. To further enhance the mechanical reinforcement of chitosan, graphene oxide (GO) has been incorporated to form hybrid matrices [20]. Moreover, this incorporation exhibits a synergistic effect, as the cytotoxicity associated with graphene oxide is reduced in the presence of chitosan [21]. GO is a unique two-dimensional nanomaterial, well known for its large surface area that enables a high drug-loading capacity, making it suitable for drug delivery applications. Its structure consists of carbon sheets decorated with oxygen-containing groups, which allow functionalization of the nanomaterial and show promising potential in biomedical applications, including scaffolds for cell proliferation and maturation, targeted drug delivery systems, and anticancer therapies [22, 23]. Despite these advantages, its effective application as a drug carrier requires surface functionalization with a biopolymer to improve biocompatibility without significantly increasing its size. Oligochitosan has emerged as a particularly promising candidate due to its solubility, biocompatibility, and ability to interact effectively with GO surfaces. In this study, we report the synthesis of OCH by gamma irradiation, followed by the functionalization of graphene oxide with oligochitosan (OCH/GO). Both OCH and OCH/GO were characterized, and their cytotoxicity was evaluated to assess their potential as drug nanoplatforms.

## Methodology

All chemicals were analytical grade and used without further purification: graphite powder (99% purity) and $NaNO_3$ from Merck; $KMnO_4$, NaOH, $H_2SO_4$, were purchased from Lab-Synth (Brazil) and $H_2O_2$ (30% w/w) from Sigma-Aldrich. All solutions were prepared with deionized water.

### Synthesis of graphene oxide: GO

The GO was synthesized using Hummer's method, with modifications [24]. Briefly 3 g of graphite powder, 3 g of $NaNO_3$ (0.04 M) and 140 mL of $H_2SO_4$ (98%) were mixed and stirred in an ice bath. Then, 18 g of $KMnO_4$ (0.11 M) was slowly added to the mixture, maintaining a temperature at approximately 35 °C for one hour. Following this step, 100 mL of deionized (DI) water was added and the solution was stirred at 90 °C. Finally, an additional 500 mL of DI water and 18 mL of $H_2O_2$ (30% w/w) were added, turning the mixture from dark brown to yellow. The resulting suspension was centrifuged (3-30KS, Sigma, Germany) at 12,000 rpm for 10 minutes, and the graphite oxide was dispersed in water and exfoliated in an ice bath using an ultrasonic cell disruptor (Desruptor 19 kHz 500 W, Unique, Brazil) to obtain the final product.

### Production of oligochitosan: OCH by irradiation

Chitin powder (400Mesh) was extracted from shrimp shells (*Macrobrachium carcinus*) and deacetylated by using NaOH solution (50% 1M) under agitation 600 rpm, at the microwave radiation-assisted batch reaction unit (2.45 GHz and 1.6 kW), for 1h at 110ºC. Chitosan powder was solubilized in acetic acid (3% w/v) and centrifuged. The gel-like product (100 g), was then subjected to gamma irradiation at absorbed dose of 40 kGy and dose rate of 9.8 kGy/h using a Gamma Chamber 5000 (GC-5000), (Bhabha Atomic Research Center (BARC). The irradiated gel-like product was freeze-dried and processed by cryogenic milling in three cycles consisting of 2 minutes of grinding, 3 minutes of freezing, and 2 minutes of grinding, at a speed of 15 cps using a Horiba Scientific horizontal mill, model Freezer/Mill 6770 [25]. Fig 1 shows the schematic representation of the process for obtaining oligochitosan.

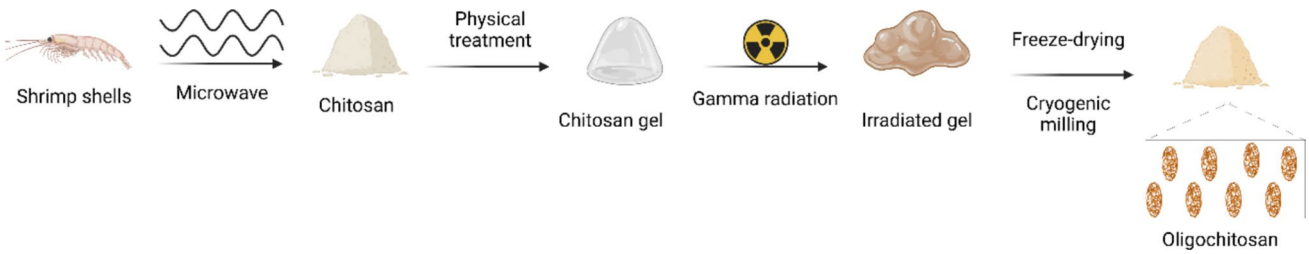


**Fig. 1** Methods for obtaining oligochitosan using gamma irradiation

### Synthesis of oligochitosan/graphene oxide (OCH/GO) nanocomposite

To synthesize OCH/GO nanocomposite, 2 mL of N-(3-dimethylaminopropyl)-N′-ethylcarbodiimide (EDC, 0.03 M) and 2 mL of N-hydroxysuccinimide (NHS, 0.06 M) were added to a 96.0 mL solution of dispersed GO (0.2 g/L) in deionized water. Then, OCH (0.25 g/L), previously dissolved in 10 mL acetic acid (1%), was added dropwise to the mixture under continuous stirring. The reaction was maintained under reflux for 1 h. Subsequently, the mixture was cooled to room temperature, dialyzed with a 14 kDa membrane for 24 h to remove residual reagents, centrifuged at 3000 rpm for 10 min and lyophilized for further characterization. The yield was 75%, obtaining a mass of nanocomposites of 37 mg of OCH/GO [26].

### Characterizations

X-ray diffraction (XRD) measurements were performed on a Rigaku X-ray diffractor, model SmartLab SE, equipped with a copper tube and scintillation detector, with counting times of 6 seconds per 0.1° step. For scanning electron microscopy (SEM) on a JEOL SM IT700HR instrument, and oligochitosan samples were gold-coated to improve resolution. The samples suspended in water were also analyzed by dynamic light scattering (DLS) using a Litesizer DLS instrument. CH and OCH were characterized by rheological measurements using a Lamy RM100 rheometer, model First Pro Plus, at 25.0 ± 0.1 °C. Solutions were prepared in an aqueous system ($CH_3COOH$ 0.10 mol/L -NaCl 0.20 mol/L), filtered through 0.45 µm membranes and subjected to low shear rates. The intrinsic viscosity ([η]) determined using the Huggins equation, and the viscosimetric average molar mass (Mv) was calculated by the Mark-Houwink-Sakurada equation, with constants $K = 1.8 \times 10^{-3}$ and $a = 0.932$ for this solvent [27, 28]. Infrared spectroscopy (FTIR) analyses were performed on a Shimadzu IRPrestige-21 spectrometer, using either KBr pellets or ATR mode, in the frequency range 4000–400 $cm^{-1}$. For topographical characterization, atomic force microscopy (AFM) was conducted using a Bruker MultiMode 8-HR instrument.

### Cell culture

Murine fibroblasts NIH/3T3 (ATCC CRL-1658) were cultured in RPMI1640 medium (Sigma-Aldrich, R6504), supplemented with fetal bovine serum (10%, Cultilab), L-glutamine and antibiotics mixture (penicillin, 10.000 UI/mL, streptomycin, 10.000 µg/mL, Gibco, 15140). Cells were seeded at 5000 cells per well (100 µL) in 96-well cell culture plates and incubated at 37 °C in a humidified atmosphere of 5% $CO_2$.

### Cell viability

Extracts were prepared suspending GO or OCH/GO in culture medium, incubating for 24 h at 37 °C, and sterilizing by filtration through 0.22µm membranes before transfer to the cultures. NIH/3T3 cells were then exposed to OCH/GO extracts (0.78–100 µg/mL, pH 6.5) for 24 h. After this period, the cells were washed with sterile phosphate-buffered saline (PBS) (pH 7.2–7.6) at 37 °C and incubated for 2 h with 100 µL of medium containing MTS (CellTiter 96® AQueous, Promega, G1112) and PMS (Sigma-Aldrich, P9625) according to the manufacturer's instructions. Absorbance at 490 nm was measured using a Multiskan EX (Thermo). Cell proliferation was expressed as % growth inhibition relative to controls and analyzed by one-way ANOVA with Bonferroni post hoc test. Negative control was untreated cells (0.9% NaCl), and positive control was latex extract (0.5 g/L, 24 h). Cell viability was calculated as: % Cell viability = 100 × (absorbance of experimental well/absorbance of untreated control well).

## Results and discussion

### Graphene oxide- GO

Typical X-ray diffractogram (XRD) of graphene oxide is present in Fig. 2 and exhibits a characteristic peak at 10.9°, corresponding to the increased interlayer spacing due to the presence of oxygen-containing functional groups. A broader peak observed around 42.4° is attributed to the spacing

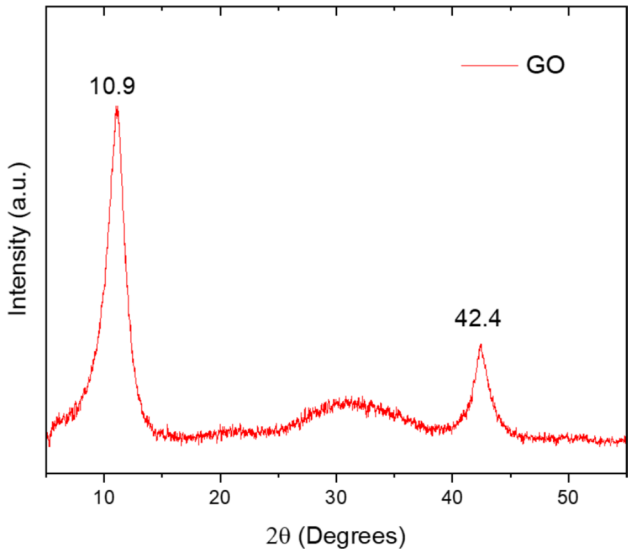


**Fig. 2** Diffractogram of synthesized graphene oxide

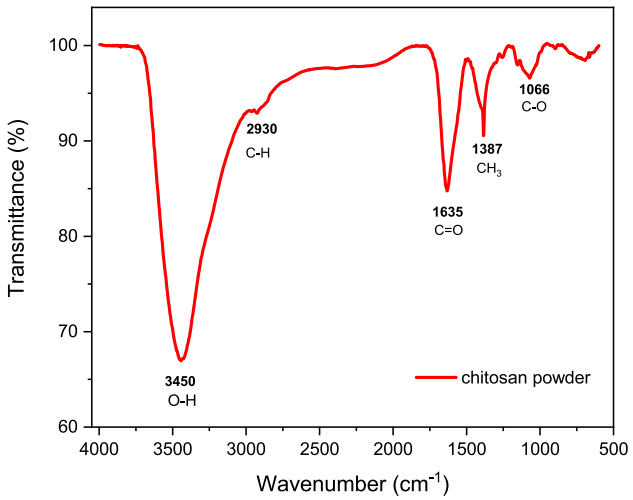


**Fig. 3** FT-IR spectrum of chitosan powder

between the carbon atoms located in the carbon network of the material [29].

## Chitosan powder

The degree of deacetylation (DG) of chitosan was determined by Fourier-transform infrared spectroscopy (FTIR) (Fig. 3), as described in the literature [31, 32]. The vibrational bands corresponding to the carbonyl group ($\nu$ C=O) of amide (≈1635 $cm^{-1}$) and the O–H stretching band at ≈ 3450 $cm^{-1}$ [30]. The DG was calculated to be 71.31% according to Equation 1

$$D = 100 \cdot \left(\frac{A1665}{A3450}\right) \quad (1)$$

The FTIR spectrum of chitosan powder after irradiation shows an intense absorption band at 3450 $cm^{-1}$, characteristic of O–H and N–H stretching vibrations. A band at 2930 $cm^{-1}$ corresponds to the symmetrical stretching vibration of –C–H, attributed to methylenes. The band located at 1635 $cm^{-1}$ is attributed to –C=O amide groups. The thin band observed at 1387 $cm^{-1}$ is due to the $CH_3$ group. Finally, the band at 1066 $cm^{-1}$ is attributed to vibrations involving C–O stretching. The number of amine groups increases in chitosan compared to chitin because chitosan is derived from chitin by a process called deacetylation, which removes acetyl groups and transforms chitin's amide groups into free amine groups. This difference in the amount of amine groups is what gives chitosan its greater solubility in acidic environments and other properties that are distinct from chitin [33].

The morphology of the chitosan powder was analyzed by scanning electron microscopy (SEM), and the image is shown in Fig. 4.

## Oligochitosan: OCH

A gamma irradiation dose of 40 kGy was selected based on previous reports [14, 34] and confirmed as optimal in our optimization studies, where the addition of (0.%) sodium hydroxide prior to irradiation yielded gel-like chitosan.

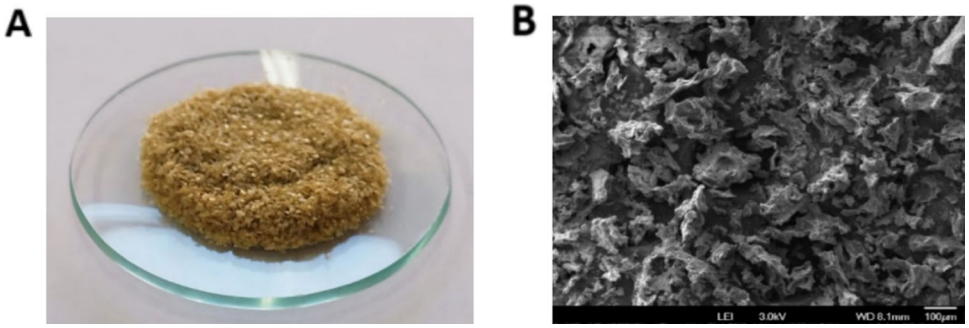


**Fig. 4** Chitosan obtained by the microwave process: **a** powder obtained after the process and **b** scanning microscopy image of the material

Although Choi reported that chitosan solubility increased above 40 kGy, the size of the products obtained under those conditions was not described. On the other hand, Pasanphan et al. [34] irradiated chitosan in colloidal form to produce chitosan nanoparticles. In the present study, irradiation of chitosan in gel form resulted in products larger than nanoparticles, with DLS analysis revealing particle sizes ranging from 1000 to 2000 nm (Fig. 5a).

This finding supports previous studies on the role of water radiolysis in chitosan degradation. In gel systems, water is confined within a three-dimensional network, whereas in colloidal systems it remains more mobile and thus more available to radiation. OH radicals generated from water radiolysis (Eq. 2) [35] efficiently cleave the β-1,4 glycosidic bonds in chitosan [36].

$$H_2O\gamma - \text{irradiation} \rightarrow e_{aq}^{-} + H^{\cdot} + HO^{\cdot} \quad (2)$$

Thus, when the chitosan gel was irradiated, polymer chain scission occurred, resulting in the formation of oligochitosans.

Due to the large variation in the size distribution of the oligochitosan, grinding was carried out to improve uniformity. This technique involves the use of liquid nitrogen to freeze the material, rendering it brittle and more susceptible to mechanical breakdown. The frozen sample is then subjected to grinding using a milling system, in repeated cycles, to achieve effective size reduction. The DLS analysis of the product showed that, in addition to a reduction in the amplitude of the size distribution, the particle diameter decreased mostly within the range of 40 and 250 nm (Fig 5b).

Morphological differences are shown in Fig. 6 through SEM images. The SEM image of irradiated gel-like chitosan (Fig. 6a) reveals characteristic oligochitosan features, while Fig. 6b shows the formation of spherical particles after the cryogenic grinding process.

Viscosity measurements of the CH and OCH samples allowed the evaluation of their molecular weights (Fig. 7). Chitosan solutions exhibit non-Newtonian behavior, characterized by a decrease in viscosity with increasing shear rate [37]. The initial molecular weight of chitosan was determined to be 243.0 kDa, which decreased to 154.2 kDa

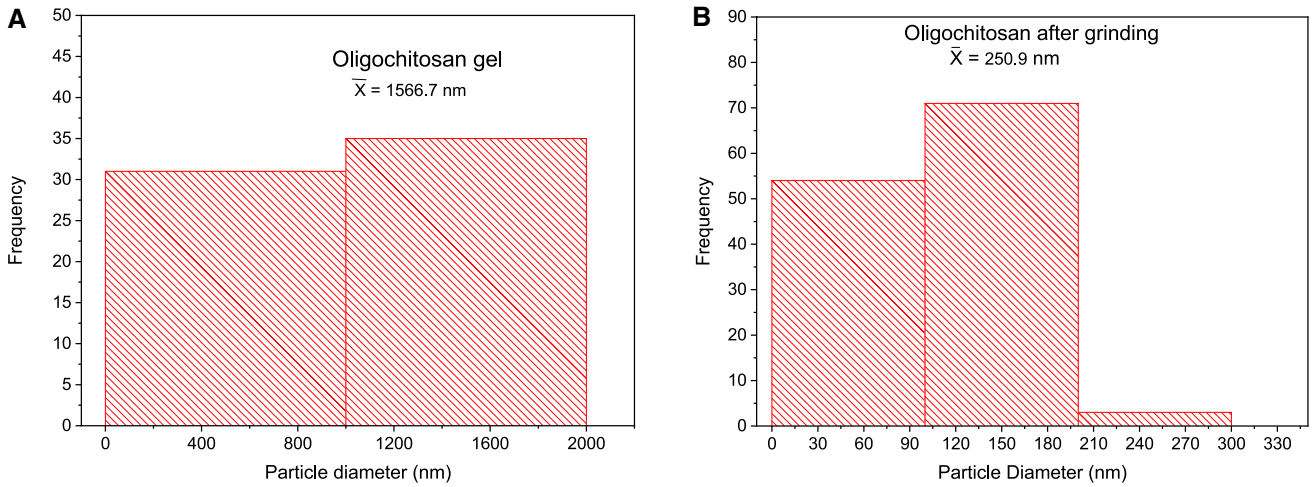


**Fig. 5** Analysis of the hydrodynamic diameter of chitosan gels irradiated with 40 kGy and a dose rate of 9.8 kGy/h: **a** before the cryogenic grinding process and **b** after cryogenic grinding process

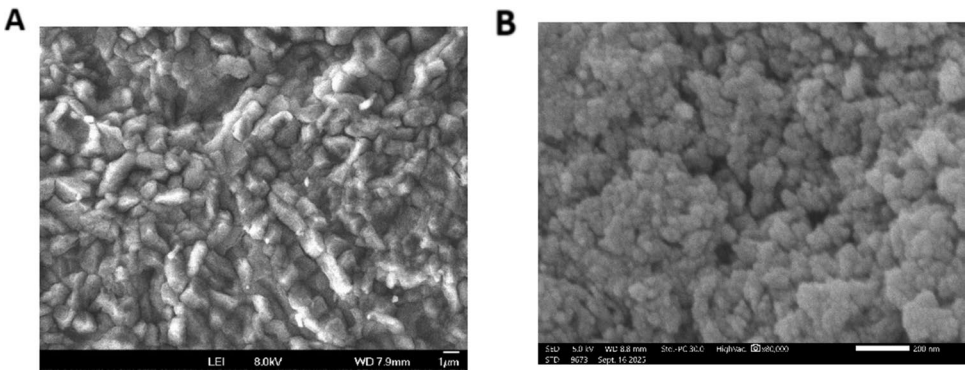


**Fig. 6** SEM images of OCH obtained by gamma radiation: **a** before grinding, without coating and **b** OCH after cryogenic grinding, with the sample coated with gold

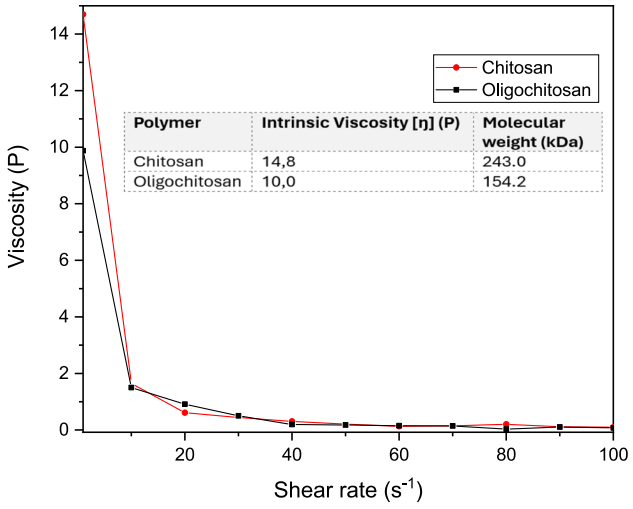


**Fig. 7** Viscosity curves of chitosan and oligochitosan solutions as a function of shear rate, at a concentration of 0.003 g/mL

following the cryogenic milling process, resulting in a reduction in viscosity [38].

## OCH/GO nanocomposite

The functionalization of graphene oxide (GO) with oligochitosan was performed via chemical amidation, using EDC/NHS as coupling agents [39]. The atomic force microscopy (AFM) analyses were employed to confirm the synthesis of the nanocomposite (Fig. 8).

The presence of oligochitosan on the graphene oxide surface was confirmed through the differences in AFM topography between the pristine graphene oxide sheets and the OCH/GO nanocomposite. While GO, as a two-dimensional nanomaterial with a uniform height profile, the OCH/GO displayed surface irregularities with height variations of up to 14 nm. This result can be attributed to the incorporation of oligochitosan on the surface of the graphene oxide sheets.

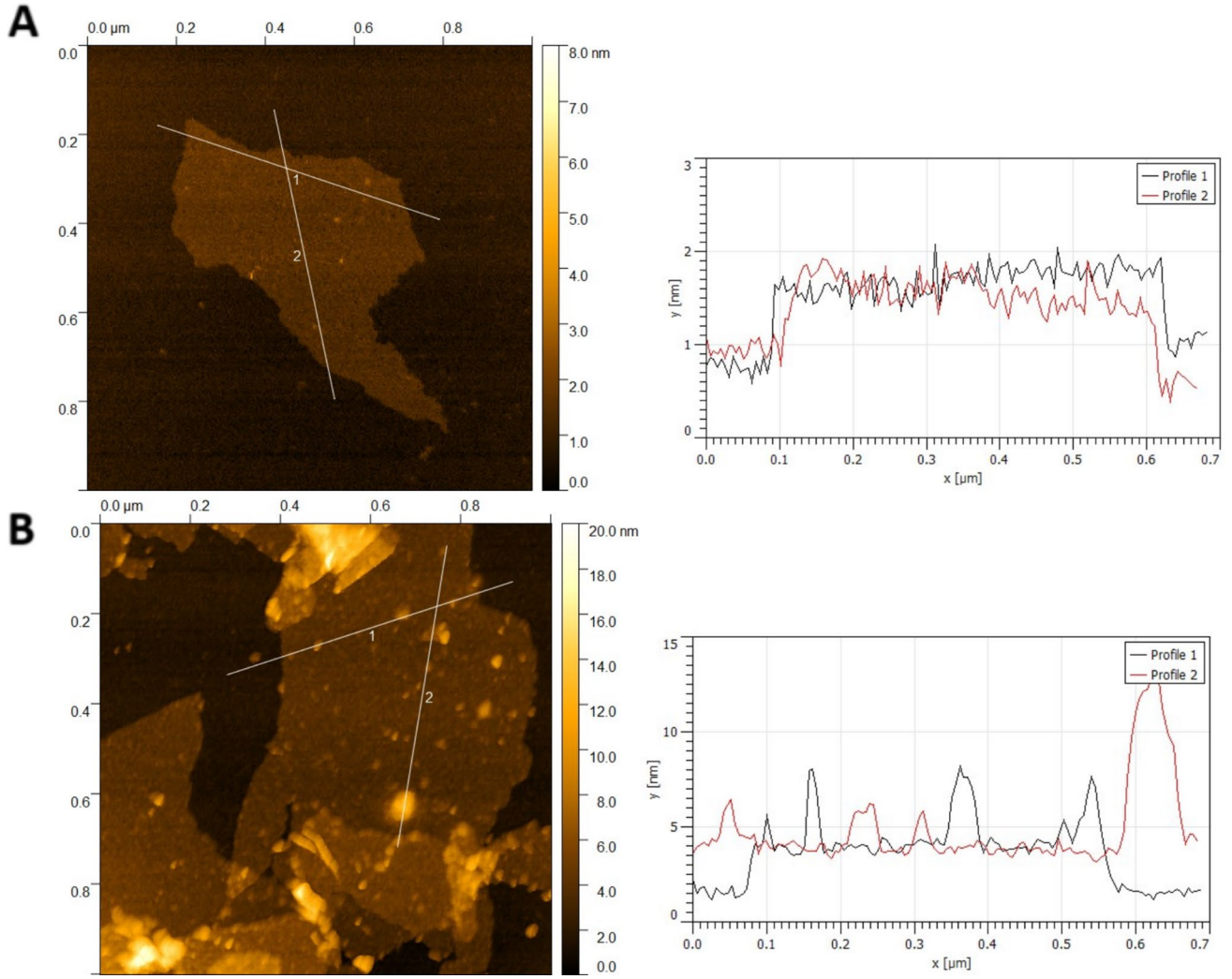


**Fig. 8** AFM topography of GO and OCH/GO: In (**a**) GO before the incorporation process and (**b**) after the process with the presence of OCH on the surface of the GO sheets

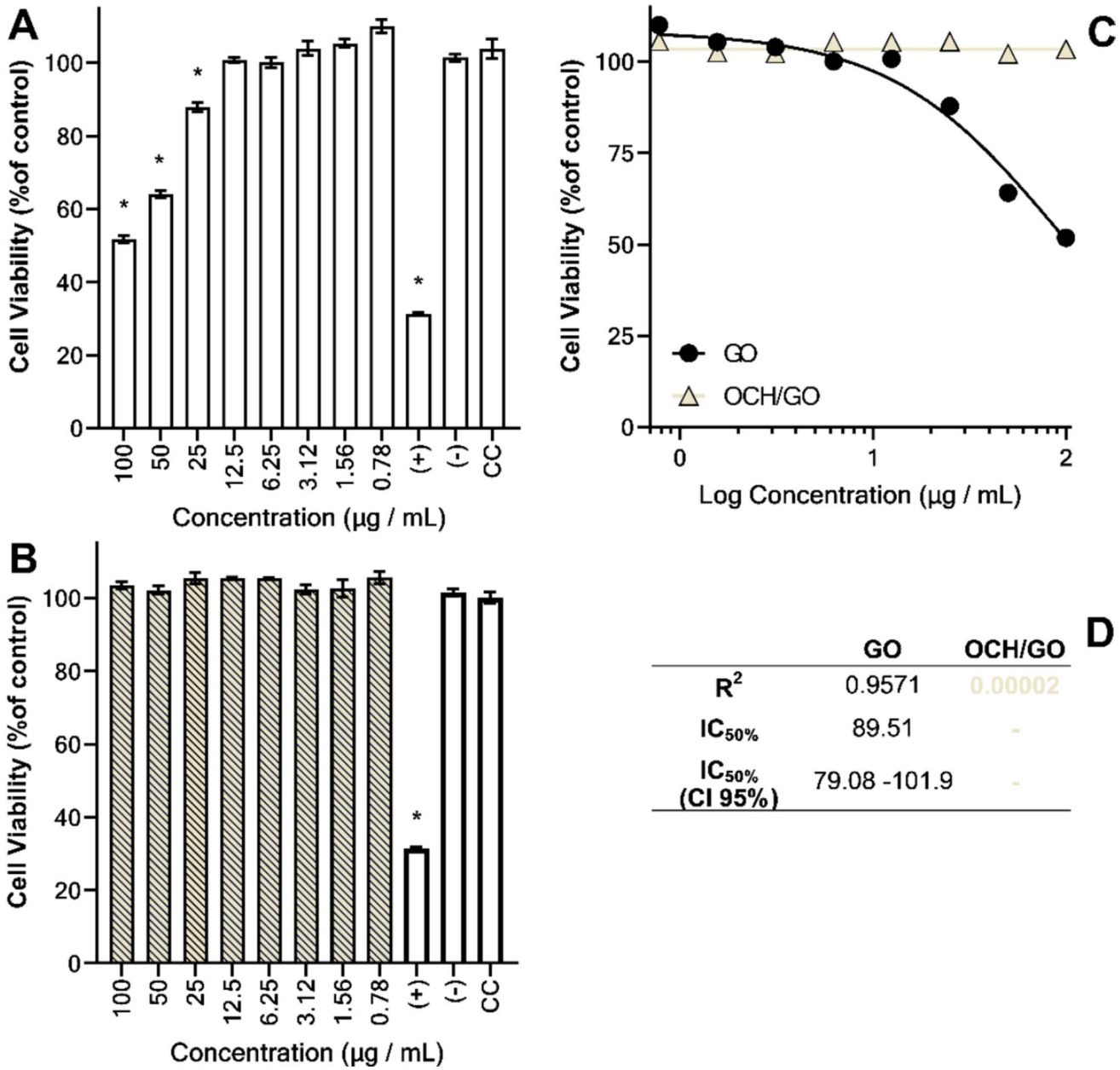


**Fig. 9** Cytotoxicity of serial dilution of extracts prepared from suspensions of GO or OCH/GO in culture medium for 24h. In (**A**) and (**B**) the cell viability values (% of cell controls) of GO and OCH/GO, respectively. Column height: means. Error bars: standard error of means (SEM). (*): $p<0.0001$ (vs.CC). In (**C**) the IC50% plot of GO (black) and OCH/GO (beige), and $R^2$ and $IC_{50\%}$ obtained values are shown in (**D**)

## Cytotoxicity test GO and OCH/GO

The cytotoxicity assays of both synthesized materials evaluated the ability to damage NIH/3T3 cells. For GO, cell toxicity can be due to several factors, including concentration, lateral size, and surface charge. Studies have shown that GO can induce cellular damage, such as membrane disruption and the production of reactive oxygen species (ROS), leading to oxidative stress characterized by an imbalance between free radicals and antioxidants [40].

Figure 9 shows the cytotoxicity tests for GO and OCH/GO. For GO alone (Fig. 9a), some concentrations showed a degree of toxicity, influencing the percentage of viable cells, and can be compared to the positive control. However, when the material is incorporated as oligochitosan (Fig. 9b), toxicity is not verified, demonstrating

biocompatibility with NIH/3T3 cells without chemical alterations considered toxic to the cell line.

GO extracts induced significant cytotoxicity compared to controls at concentrations of 100, 50, and 25 µg/mL, and OCH/GO extracts did not do so at any concentration, showing that chitosan incorporation protected cells from GO-induced cell death. Cytotoxicity induced by graphene oxide nanostructures can manifest through several mechanisms, related to factors such as GO concentration, duration of exposure, and cell type affected [41]. Disruption of cytoplasmic membranes represents the main mode of graphene oxide-induced toxicity, resulting from the direct physical interaction of GO nanosheets with the lipid bilayer, leading to membrane destabilization and, therefore, compromising cell integrity [42]. This interaction can also initiate some events, including the leakage of intracellular components and the influx of extracellular substances, eventually leading to cell death [43]. Furthermore, the internalization of graphene oxide nanostructures can induce the accumulation of reactive oxygen species (ROS) inside cells [44] and lysosomal dysfunction [45].

Despite its insolubility in aqueous medium, graphene oxide nanosheets may find high diversity of biomolecules in mammalian cell culture medium that can induce a variety of surface modifications and interactions [46, 47].

Coating graphene oxide nanosheets with chitosan can confer to the resulting nanocomposite material enhanced biocompatibility, reduced cytotoxicity, and improved cellular interactions, promoting suggestions of its safe and effective utilization in various biomedical applications [41]. Chitosan's inherent biocompatibility is originated from its structural similarity to glycosaminoglycans, naturally found in the extracellular matrix of mammalian tissues [48]. This mimicry leads to a highly well successful integration of chitosan-based materials with biological systems, reducing adverse reactions and improving cellular adhesion and proliferation. Furthermore, the presence of chitosan coating can effectively cover eventual sharp edges and hydrophobic surfaces of graphene oxide nanosheets, which are known to induce cellular damage and inflammatory responses. The experiments above demonstrated that OCH/GO did not induce cytotoxicity at any of the concentrations, presenting biocompatibility with NIH/3T3 cells without chemical alterations considered toxic to the studied cell line. Furthermore, chitosan has intrinsic antimicrobial and chelating properties, which contribute to the application of this nanocomposite in biological uses, such as the creation of hydrogels and scaffolds for tissue regeneration, or even in the encapsulation of drugs [49, 50].

## Conclusions

Oligochitosan was obtained from chitosan by gamma irradiation at an absorbed dose of 40 kGy and a dose rate of 9.8 kGy/h, yielding a size distribution ranging from 1000 to 2000 nm. To incorporate into graphene oxide and enhance the solubility of the nanocomposite, a top-down approach using cryogenic milling was employed to further reduce the particle size of chitosan. The resulting oligomers exhibited sizes in the range of 150–250 nm, with a narrower size distribution and a molecular weight of 154.2 kDa. The OCH/GO nanocomposite was subsequently characterized by atomic force microscopy (AFM) topography. Cytotoxicity assays confirmed the absence of toxic effects, demonstrating that the incorporation of oligochitosan into graphene oxide improved its biocompatibility and reinforced its potential for applications in tissue engineering. This study highlights the feasibility of employing oligochitosan/graphene oxide nanocomposites for biomedical applications.

**Acknowledgements** The authors gratefully acknowledge the financial support provided by the National Council for Scientific and Technological Development (CNPq) and the Ministry of Science, Technology, and Innovation (MCTI), Brazil in the framework of CNPq/MCTI-INOVA 408501/2022-7, and the National Council for the Improvement of Higher Education (CAPES) for the fellowship. This research used facilities of the Brazilian Nanotechnology National Laboratory (LNNano), part of the Brazilian Centre for Research in Energy and Materials (CNPEM), a private non- profit organization under the supervision of the Brazilian Ministry for Science, Technology, and Innovations (MCTI). The Atomic Force Microscope staff are acknowledged for their assistance during the experiments AFM 20242253, respectively.

## References

1. Asthana N, Pal K, Khan A, Malik A (2024) Novel biopolymeric materials potential utilization for environmental practices. J Mol Struct. https://doi.org/10.1016/j.molstruc.2024.138390
2. Aranaz I, Alcántara AR, Civera MC, Arias C, Elorza B, Heras Caballero A, Acosta N (2021) Chitosan: an overview of its properties and applications. Polym J. https://doi.org/10.3390/polym13193256
3. Nicola R, Grosso C, Delerue-Matos C (2024) Shrimp waste upcycling: unveiling the potential of polysaccharides, proteins, carotenoids, and fatty acids with emphasis on extraction techniques and bioactive properties. Mar Drugs. https://doi.org/10.3390/md22040153
4. Amiri H, Aghbashlo M, Sharma M, Gaffey J, Manning L, Moosavi BSM, Tabatabaei M (2022) Chitin and chitosan derived from crustacean waste valorization streams can support food systems and the UN sustainable development goals. Nat Food. https://doi.org/10.1038/s43016-022-00591-y
5. Saiyad M, Shah N, Joshipura M, Dwivedi A, Pillai S (2024) Chitosan and its derivatives in wastewater treatment application. Mater Today Proc. https://doi.org/10.1016/j.matpr.2023.10.157

6. Planas A, Biarnés X, Hamer SN, Cord-Landwehr S, Waegeman H, Moerschbacher BM, Kolkenbrock S (2015) Enzymatic production of defined chitosan oligomers with a specific pattern of acetylation using a combination of chitin oligosaccharide deacetylases. Sci Rep. https://doi.org/10.1038/srep08716
7. Kaczmarek MB, Struszczyk-Swita K, Li X, Szczęsna-Antczak M, Daroch M (2019) Enzymatic modifications of chitin, chitosan, and chitooligosaccharides. Front Bioeng Biotechnol. https://doi.org/10.3389/fbioe.2019.00243
8. Nguyen THP, Le NAT, Tran PT, Du Bui D, Nguyen QH (2023) Preparation of water-soluble chitosan oligosaccharides by oxidative hydrolysis of chitosan powder with hydrogen peroxide. Heliyon. https://doi.org/10.1016/j.heliyon.2023.e19565
9. Gryczka U, Dondi D, Chmielewski AG, Migdal W, Buttafava A, Faucitano A (2009) The mechanism of chitosan degradation by gamma and e-beam irradiation. Radiat Phys Chem. https://doi.org/10.1016/j.radphyschem.2009.03.081
10. Ashfaq A, Clochard MC, Coqueret X, Dispenza C, Driscoll MS, Ulański P, Al-Sheikhly M (2020) Polymerization reactions and modifications of polymers by ionizing radiation. Polym J. https://doi.org/10.3390/polym12122877
11. Hien NQ, Van Phu D, Duy NN, Lan NTK (2012) Degradation of chitosan in solution by gamma irradiation in the presence of hydrogen peroxide. Carbohydr Polym. https://doi.org/10.1016/j.carbpol.2011.08.018
12. Hai L, Diep TB, Nagasawa N, Yoshii F, Kume T (2003) Radiation depolymerization of chitosan to prepare oligomers. Nucl Instrum Methods Phys. https://doi.org/10.1016/S0168-583X(03)01181-9
13. Kang B, Dai YD, Zhang HQ, Chen D (2007) Synergetic degradation of chitosan with gamma radiation and hydrogen peroxide. Polym Degrad Stabil. https://doi.org/10.1016/j.polymdegradstab.2006.12.006
14. Choi WS, Ahn KJ, Lee DW, Byun MW, Park HJ (2002) Preparation of chitosan oligomers by irradiation. Polym Degrad Stabil. https://doi.org/10.1016/S0141-3910(02)00226-4
15. Ahmed KBM, Khan MMA, Siddiqui H, Jahan A (2020) Chitosan and its oligosaccharides, a promising option for sustainable crop production- a review. Carbohydr Polym. https://doi.org/10.1016/j.carbpol.2019.115331
16. Muanprasat C, Chatsudthipong V (2017) Chitosan oligosaccharide: biological activities and potential therapeutic applications. Pharmacol Ther. https://doi.org/10.1016/j.pharmthera.2016.10.013
17. Naveed M, Phil L, Sohail M, Hasnat M, Baig MMFA, Ihsan AU, Zhou QG (2019) Chitosan oligosaccharide (COS): an overview. Int J Biol Macromol. https://doi.org/10.1016/j.ijbiomac.2019.01.192
18. Phan TTV, Phan DT, Cao XT, Huynh TC, Oh J (2021) Roles of chitosan in green synthesis of metal nanoparticles for biomedical applications. Nanomater. https://doi.org/10.3390/nano11020273
19. Lu B, Wang CF, Wu DQ, Li C, Zhang XZ, Zhuo RX (2009) Chitosan based oligoamine polymers: synthesis, characterization, and gene delivery. J Control Release. https://doi.org/10.1016/j.jconrel.2009.03.004
20. Zuo PP, Feng HF, Xu ZZ, Zhang LF, Zhang YL, Xia W, Zhang WQ (2013) Fabrication of biocompatible and mechanically reinforced graphene oxide-chitosan nanocomposite films. Chem Cent J. https://doi.org/10.1186/1752-153X-7-39
21. Farani MR, Zare I, Mirshafiei M, Gholami A, Zhang M, Pishbin E, Huh YS (2025) Graphene oxide-engineered chitosan nanoparticles: Synthesis, properties, and antibacterial activity for tissue engineering and regenerative medicine. Chem Eng J. https://doi.org/10.1016/j.cej.2025.160852
22. Mousavi SM, Low FW, Hashemi SA, Lai CW, Ghasemi Y, Soroshnia S, Tiong SK (2020) Development of graphene-based nanocomposites towards medical and biological applications. Artif Cells Nanomed Biotechnol. https://doi.org/10.1080/21691401.2020.1817052
23. Amiryaghoubi N, Fathi M, Barar J, Omidian H, Omidi Y (2022) Recent advances in graphene-based polymer composite scaffolds for bone/cartilage tissue engineering. J Drug Deliv Sci Technol. https://doi.org/10.1016/j.jddst.2022.103360
24. Hummers, Offeman RE (1958) Preparation of graphitic oxide. J Am Chem Soc. https://doi.org/10.1021/ja01539a017
25. Mukherjee S, Cord-Landwehr S, Rani TS, Duhsaki L, Sarma SS, Rao TN, Madhuprakash J (2025) First evidence of cryo-milling enhancing enzymatic production of chitooligosaccharides from chitin biomass. Carbohydr Polym. https://doi.org/10.1016/j.carbpol.2025.123509
26. Depan D, Pesacreta TC, Misra RDK (2014) The synergistic effect of a hybrid graphene oxide–chitosan system and biomimetic mineralization on osteoblast functions. Biomater Sci. https://doi.org/10.1039/C3BM60192G
27. Popescu R, Dinu-Pîrvu CE, Ghica MV, Anuța V, Popa L (2024) Physico-chemical characterization and initial evaluation of carboxymethyl chitosan-hyaluronan hydrocolloid systems with insulin intended for intranasal. Int J Mol Sci. https://doi.org/10.3390/ijms251910452
28. Roberts GA, Domszy JG (1982) Determination of the viscometric constants for chitosan International. Biol Macromol. https://doi.org/10.1016/01418130(82)90074-5
29. Jiao X, Qiu Y, Zhang L, Zhang X (2017) Comparison of the characteristic properties of reduced graphene oxides synthesized from natural graphites with different graphitization degrees. RSC Adv. https://doi.org/10.1039/C7RA10809E
30. Dong Y, Xu C, Wang J, Wang M, Wu Y, Ruan Y (2001) Determination of degree of substitution for N-acylated chitosan using IR spectra. Sci China B Chem. https://doi.org/10.1007/BF02879541
31. Brugnerotto J, Lizardi J, Goycoolea FM, Argüelles-Monal W, Desbrieres J, Rinaudo M (2001) An infrared investigation in relation with chitin and chitosan characterization. Polym J. https://doi.org/10.1016/S0032-3861(00)00713-8
32. Sierra DME, Orozco CPO, Rodríguez MAQ, Villa WAO (2013) Optimización de un protocolo de extracción de quitina y quitosano desde caparazones de crustáceos. Scientia et technica. https://doi.org/10.22517/23447214.7555
33. Chmielewski AG (2010) Chitosan and radiation chemistry. Radiat Phys Chem. https://doi.org/10.1016/j.radphyschem.2009.11.002
34. Pasanphan W, Buettner GR, Chirachanchai S (2008) Chitosan conjugated with deoxycholic acid and gallic acid: a novel biopolymer-based additive antioxidant for polyethylene. J Appl Polym Sci. https://doi.org/10.1002/app.27953.2023.109670
35. Pasanphan W, Rimdusit P, Choofong S, Piroonpan T, Nilsuwankosit S (2010) Systematic fabrication of chitosan nanoparticle by gamma irradiation. Radiat Phys Chem. https://doi.org/10.1016/j.radphyschem.2010.04.003
36. Hamill WH (1969) Model for the radiolysis of water. J Phys Chem. https://doi.org/10.1021/j100725a027
37. Ulanski P, von Sonntag C (2000) OH-Radical-induced chain scission of chitosan in the absence and presence of dioxygen. J Chem Soc. https://doi.org/10.1039/b003952g
38. Carrera C, Bengoechea C, Carrillo F, Calero N (2023) Effect of deacetylation degree and molecular weight on surface properties of chitosan obtained from biowastes. Food Hydrocoll. https://doi.org/10.1016/j.foodhyd.2022.108383
39. Parsamehr PS, Zahed M, Tofighy MA, Mohammadi T, Rezakazemi M (2019) Preparation of novel cross-linked graphene oxide membrane for desalination applications using (EDC and NHS)-activated graphene oxide and PEI. Desalination. https://doi.org/10.1016/j.desal.2019.114079
40. Emadi F, Amini A, Gholami A, Ghasemi Y (2017) Functionalized graphene oxide with chitosan for protein nanocarriers to protect

against enzymatic cleavage and retain collagenase activity. Sci Rep. https://doi.org/10.1038/srep42258
41. Shin YC, Song SJ, Hong SW, Jeong SJ, Chrzanowski W, Lee JC, Han DW (2017) Multifaceted biomedical applications of functional graphene nanomaterials to coated substrates patterned arrays and hybrid Scaffolds. Nanomater. https://doi.org/10.3390/nano7110369
42. Perez J E, Alsharif N, Martinez Banderas A, Othman B, Merzaban J, Ravasi T, Kosel J (2018) Review of in vitro toxicity of nanoparticles and nanorods: Part 1. Cytotoxicity. In: Çelik TA (ed) Cytotoxicity. https://doi.org/10.5772/intechopen.76365
43. Egorova MN, Tarasova LA, Vasilieva FD, Akhremenko YA, Smagulova SA (2018) Antimicrobial activity of graphene oxide sheets. AIP Conf Proc. https://doi.org/10.1063/1.5079359
44. Lammel T, Navas JM (2014) Graphene nanoplatelets spontaneously translocate into the cytosol and physically interact with cellular organelles in the fish cell line PLHC-1. Aquat Toxicol. https://doi.org/10.1016/j.aquatox.2014.02.016
45. Wang F, Bexiga MG, Anguissola S, Boya P, Simpson JC, Salvati A, Dawson KA (2013) Time resolved study of cell death mechanisms induced by amine-modified polystyrene nanoparticles. Nanoscale. https://doi.org/10.1039/c3nr03249c
46. Winzen S, Schoettler S, Baier G, Rosenauer C, Mailaender V, Landfester K, Mohr K (2015) Complementary analysis of the hard and soft protein corona: sample preparation critically effects corona composition. Nanoscale. https://doi.org/10.1039/C4NR05982D
47. Shende P, Augustine S, Prabhakar B (2020) A review on graphene nanoribbons for advanced biomedical applications. Carbon Lett. https://doi.org/10.1007/s42823-020-00125-1
48. Xie H, Cao T, Rodríguez-Lozano FJ, Luong-Van EK, Rosa V (2017) Graphene for the development of the next-generation of biocomposites for dental and medical applications. Dent Mater. https://doi.org/10.1016/j.dental.2017.04.008
49. Zhang M, Zhang F, Li C, An H, Wan T, Zhang P (2022) Application of chitosan and its derivative polymers in clinical medicine and agriculture. J Polym. https://doi.org/10.3390/polym14050958
50. Nandhini R, Rajeswari E, Harish S, Sivakumar V, Gangai Selvi R (2025) Role of chitosan nanoparticles in sustainable plant disease management. J Nanopart Res. https://doi.org/10.1007/s11051-024-06203-z



## Authors and Affiliations

**Karina de Oliveira Gonçalves[1] · Miguel Duarte[1] · Daniel Perez Vieira[2] · Sumair Gouveia Araújo[3] · Liliane Landini[3] · Solange Kazumi Sakata[1]**

✉ Solange Kazumi Sakata
sksakata@ipen.br

[1] Radiation Technology Center, Nuclear and Energy Research Institute, 1IPEN/USP. Prof. Lineu Prestes Ave., 2242, University City, São Paulo, SP 05508-000, Brazil

[2] Biotechnology Center, Nuclear and Energy Research Institute, 1IPEN/USP. Prof. Lineu Prestes Ave., 2242, University City, São Paulo, SP 05508-000, Brazil

[3] Center for Chemistry and Environment, Nuclear and Energy Research Institute, 1IPEN/USP. Prof. Lineu Prestes Ave., 2242, University City, São Paulo, SP 05508-000, Brazil